3816 *Chem. Mater.* **2009,** *21,* 3816–3822
DOI:10.1021/cm901197s

CHEMISTRY OF MATERIALS
Article

# Fluorescent Single-Molecular Core−Shell Nanospheres of Hyperbranched Conjugated Polyelectrolyte for Live-Cell Imaging

Kan-Yi Pu, Kai Li, Jianbing Shi, and Bin Liu*

*Department of Chemical and Biomolecular Engineering, 4 Engineering Drive 4, National University of Singapore, Singapore 117576*

*Received May 4, 2009. Revised Manuscript Received July 15, 2009*

A water-soluble fluorescent hyperbranched conjugated polyelectrolyte (HCPE) with a unique double-layered architecture is synthesized via the combination of alkyne polycyclotrimerization and alkyne-azide "click" reaction for live-cell imaging. Because of the rigid conjugated core that offers shape persistence, and the water-soluble nonionic poly(ethylene glycol) shells that passivate the macromolecular surface, HCPE intrinsically forms single-molecular core−shell nanospheres with an average diameter of ∼10.7 nm and a narrow size distribution of ∼1.5, according to transmission electron microscopy images. The resulted organic nanospheres possess high quantum yield (30% in buffer), good solution stability, and low cytotoxicity. Using breast cancer cell MCF-7 as an example, these core−shell nanospheres are internalized efficiently by the cells and accumulated in the cytoplasm to give bright fluorescence. Photostability study reveals that these nanospheres are significantly more stable than commercial dyes, such as fluorescein, rhodamine, and Cy5, which demonstrates the great potential of organic polymeric nanomaterials in long-term clinical applications. In addition, the state-of-the-art synthetic methods used herein provide the feasibility and flexibility to modify both core and shell components of HCPE for specific biological applications.

## Introduction

A vital challenge in cell biology and biochemistry is to decipher celluar structures, behaviors, and physiological functions through visual methods involving minimal perturbation to the biological system.[1] During the past decades, fluorescent tagging has been proven to be a powerful implement for cell imaging both in vitro and in vivo.[2] Because small fluorophores and fluorescent proteins suffer from low photobleaching thresholds that limit their effectiveness in long-term and three-dimensional imaging,[3] semiconductor quantum-dots (QDs) have emerged as a category of bright and photostable alternatives.[4] However, QDs tend to aggregate and lose their luminescence in intracellular environments, even under acidic (pH < 5) or isotonic conditions.[5] Moreover, the intrinsically toxic elements within QDs, such as cadmium and selenium, are liable to release and in turn render toxicity to both cell cultures and live organisms, especially in radiation-caused oxidation environment.[6] Although surface modification of QDs with biomolecules or biocompatible polymers could mitigate these detrimental problems, this strategy is complicated and time-consuming. More importantly, surface modification often has a negative impact on the luminescence and dimension of QDs.[7] As a consequence, novel fluorescent nanomaterials with good photostability and biocompatibility remain in urgent demand for cell imaging.

Conjugated polyelectrolytes (CPEs) are fluorescent macromolecules with electron-delocalized backbone and water-soluble side chains.[8] Superior to small molecule fluorophores, CPEs have larger absorption cross sections and higher fluorescence.[9] Although CPEs have formed an excellent basis for chemical and biological sensors,[10] their exploitation in cell imaging is seldom reported, possibly because of the linear geometries of

*Corresponding author. E-mail: cheliub@nus.edu.sg.

(1) (a) Weissleder, R. *Science* **2006**, *312*, 1168–1170. (b) Jaiswal, J. K.; Simon, S. M. *Nat. Chem. Biol.* **2007**, *3*, 92–98. (c) Morris, D. M.; Jensen, G. J. *Annu. Rev. Biochem.* **2008**, *77*, 583–613.
(2) Jaiswal, J. K.; Mattoussi, H.; Mauro, J. M.; Simon, S. M. *Nat. Biotechnol.* **2003**, *21*, 47–51.
(3) Lichtman, J. W.; Conchello, J. A. *Nat. Methods* **2005**, *2*, 910–919.
(4) (a) Michalet, X.; Pinaud, F. F.; Bentolila, L. A.; Tsay, J. M.; Doose, S.; Li, J. J.; Sundaresan, G.; Wu, A. M.; Gambhir, S. S.; Weiss, S. *Science* **2005**, *307*, 538–544. (b) Medintz, I. L.; Uyede, H. T.; Goldman, E. R.; Mattoussi, H. *Nat. Mater.* **2005**, *4*, 435–446.
(5) (a) Warner, J. H.; Hoshino, A.; Yamamoto, K.; Tilley, R. D. *Angew. Chem., Int. Ed.* **2005**, *44*, 4550–4554. (b) Erogbogbo, F.; Yong, K.; Roy, I.; Xu, G. X.; Prasad, P. N.; Swihart, M. T. *ACS Nano* **2008**, *2*, 873–878.
(6) (a) Derfus, A. M.; Chan, W. C. W.; Bhatia, S. N. *Nano Lett.* **2004**, *4*, 11–18. (b) Ryman-Rasmussen, J. P.; Riviere, J. E.; Monteiro-Riviere, N. A. *Nano Lett.* **2007**, *7*, 1344–1348.
(7) (a) Sinani, V. A.; Koktysh, D. S.; Yun, B. G.; Matts, R. L.; Pappas, T. C.; Motamedi, M.; Thomas, S. N.; Kotov, N. A. *Nano Lett.* **2003**, *3*, 1177–1182. (b) Kirchner, C.; Liedl, T.; Kudera, S.; Pellegrino, T.; Javier, A. M.; Gaub, H. E.; Stolzle, S.; Fertig, N.; Parak, W. J. *Nano Lett.* **2005**, *5*, 331–338.
(8) Liu, B.; Bazan, G. C. *Chem. Mater.* **2004**, *16*, 4467–4476.
(9) McQuade, D. T.; Pullen, A. E.; Swager, T. M. *Chem. Rev.* **2000**, *100*, 2537–2574.
(10) (a) Thomas, S. W.III; Joly, G. D.; Swager, T. M. *Chem. Rev.* **2007**, *107*, 1339–1386. (b) Herland, A.; Inganäs, O. *Macromol. Rapid Commun.* **2007**, *28*, 1703–1713. (c) Bazan, G. C. *J. Org. Chem.* **2007**, *72*, 8615–8635. (d) Ho, H. A.; Najari, A.; Leclerc, M. *Acc. Chem. Res.* **2008**, *41*, 168–178. (e) Pu, K. Y.; Liu, B. *Biosens. Bioelectron.* **2009**, *24*, 1067–1073.


Published on Web 08/03/2009

most CPEs that affect cellular uptake process.[11] Recently, phase-inversion precipitation of organo-soluble conjugated polymers (CP) has been employed to create CP nanoparticles for cell imaging.[12] However, these nanoparticles are in principle generated from a molecular aggregation process, in which it is difficult to control the size and size distribution. In addition, these nanoparticles do not possess cytocompatible and amendable peripheral surfaces because of their single ingredient composition,[12] leading to the restricted scope for biological imaging.

Hyperbranched macromolecules are intriguing nanoobjects that combine the advantages of spherical particles and polymers to mimic the structures and functions of globular biomolecules for biological and therapeutic applications.[13] In particular, the molecular dimensions of such "soft nanoparticles" are mainly determined by the segmental flexibility and the number of generation, enabling to fabricate single-molecular nanoparticles with tunable diameters.[14] As compared to their linear counterparts, hyperbranched conjugated polymers possess much higher photostability, as witnessed by their stabilized emission and elongated lifetime in light-emitting diodes.[15] Although many hyperbranched conjugated polymers have been reported in the literature,[16] their water-soluble counterparts are rarely developed. It occurs to us that water-soluble hyperbranched conjugated polymers could serve as a new generation of highly fluorescent and photostable organic nanospheres, which integrate the optical properties of CPEs with the cell-permeability of nanoparticles for biological imaging.

In this contribution, we design and synthesize a fluorescent hyperbranched conjugated polyelectrolyte (HCPE) with a unique core−shell structure for cell imaging (Scheme 1). Because the condensation polymerization of $AB_3$-type monomers or copolymerization of $A_2$ monomers with $B_3$ comonomers based on Pd-catalyzed coupling reactions for synthesis of hyperbranched conjugated polymers share the drawback of poorly controlled growth of propagating species,[16] we take advantage of alkyne polycyclotrimerization[17] in concert with alkyne-azide "click" chemistry[18] to prepare HCPE

**Scheme 1. Schematic Illustration of Chemical Structure of HCPE**

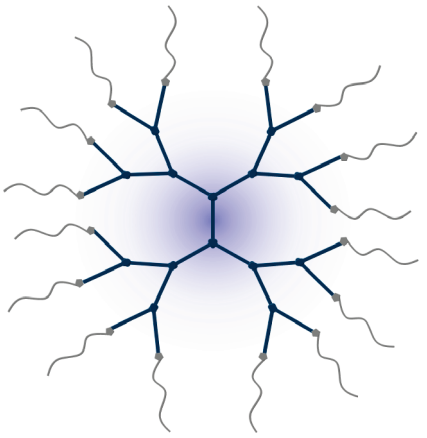

with a core−shell molecular architecture in an efficient and convenient manner. Hyperbranched cationic polyfluorene (PF) constitutes the core component of the HCPE to serve as a stable light-emitting center, whereas linear poly(ethylene glycol) (PEG) covers the periphery of the HCPE to passivate the macromolecular surface and in the meanwhile provide good cytocompatibility. Because of the three-dimensionality and shape persistence of the rigid core, the HCPE molecules form single-molecular nanospheres to facilitate the uptake process for cell imaging.

## Experimental Section

**Characterization.** Nuclear magnetic resonance (NMR) spectra were collected on Bruker Avance 500 (DRX 500, 500 MHz). Matrix-assisted laser desorption/ionization Time-of-flight (MALDI-TOF) was performed by using 2,5-dihydroxybenzoic acid (DHB) as the matrix under the reflector mode for data acquisition. Element analysis was performed on Perkin-Elmer 2400 CHN/CHNS and Eurovector EA3000 Elemental Analyzers. UV−vis spectra were recorded on a Shimadzu UV-1700 spectrometer. Photoluminescence (PL) measurements were carried out on a Perkin-Elmer LS-55 equipped with a xenon lamp excitation source and a Hamamatsu (Japan) 928 PMT, using 90° angle detection for solution samples. Fisher brand regenerated cellulose dialysis tubing with 3.5 kDa molecular weight cutoff was used for polymer dialysis. Freeze-drying was performed using Martin Christ Model Alpha 1−2/LD. Dynamic light scattering (DLS) was performed on Malvern Zetasizer Nano Series at 25 °C, and the data were analyzed by Dispersion Technology Software 5.0. High-resolution transmission electron microscopy (HR-TEM) images were obtained from a JEOL JEM-2010 transmission electron microscope with an accelerating voltage of 200 kV. The particle size and distribution were calculated by using ImageJ software.[19] All UV and PL spectra were collected at 24 ± 1 °C. Milli-Q water (18.2 MΩ) was used for all the experiments.

**Materials.** Fetal bovine serum (FBS) was purchased from Gibco (Lige Technologies, Ag, Switzerland). 3-(4,5-Dimethylthiazol-2-yl)-2,5-diphenyl tetrazolium bromide (MTT) and penicillin-streptomycin solution were purchased from

(11) Kim, I. K.; Shin, H.; Garcia, A. J.; Bunz, U. H. F. *Bioconjugate Chem.* **2007**, *18*, 815–820.
(12) (a) Moon, J. H.; McDaniel, W.; Maclean, P.; Hancock, L. F. *Angew. Chem., Int. Ed.* **2007**, *46*, 8223–8225. (b) Yao, J. H.; Mya, K. Y.; Shen, L.; He, B. P.; Li, L.; Li, Z. H.; Chen, Z. K.; Li, X.; Loh, K. P. *Macromolecules* **2008**, *41*, 1438–1443. (c) Wu, C.; Bull, B.; Szymanski, C.; Christensen, K.; McNeill, J. *ACS Nano* **2008**, *2*, 2415–2423.
(13) Zeng, F.; Zimmerman, S. C. *Chem. Rev.* **1997**, *97*, 1681–1712.
(14) Bosman, A. W.; Janssen, H. M.; Meijer, E. W. *Chem. Rev.* **1999**, *99*, 1665–1688.
(15) (a) Tao, X. T.; Zhang, Y. D.; Wada, T.; Sasabe, H.; Suzuki, H.; Watanabe, T.; Miyata, S. *Adv. Mater.* **1998**, *10*, 226–230. (b) Sun, M.; Li, J.; Li, B.; Fu, Y.; Bo, Z. *Macromolecules* **2005**, *38*, 2651–2658. (c) Paul, G. K.; Mwaura, J.; Argun, A. A.; Taranekar, P.; Reynolds, J. R. *Macromolecules* **2006**, *39*, 7789–7792.
(16) Lo, S. C.; Burn, P. L. *Chem. Rev.* **2007**, *107*, 1097–1166.
(17) (a) Peng, H.; Cheng, L.; Luo, J.; Xu, K.; Sun, Q.; Dong, Y.; Salhi, F.; Lee, P. P. S.; Chen, J.; Tang, B. Z. *Macromolecules* **2002**, *35*, 5349–5351. (b) Haussler, M.; Tang, B. Z. *Adv. Polym. Sci.* **2007**, *209*, 1–58. (c) Tang, B. Z. *Macromol. Chem. Phys.* **2008**, *209*, 1303–1307.
(18) (a) Nandivada, H.; Jiang, X.; Lahann, J. *Adv. Mater.* **2007**, *19*, 2197–2208. (b) Gramlich, P. M. E.; Wirges, C. T.; Manetto, A.; Carell, T. *Angew. Chem., Int. Ed.* **2008**, *47*, 8350–8358.
(19) Abramoff, M. D.; Magelhaes, P. J.; Ram, S. J. *J. Biophoton. Int.* **2004**, *11*(7), 36–42.

Sigma-Aldrich. Dulbecco's modified essential medium (DMEM) was a commercial product of National University Medical Institutes (Singapore). Phosphate-buffer saline (PBS; 10×) buffer with pH 7.4 (ultrapure grade) is a commercial product of first BASE Singapore. Milli-Q water (18.2 MΩ) was used to prepare the buffer solutions from the 10 × PBS stock buffer. PBS (1×) contains NaCl (137 mM), KCl (2.7 mM), $Na_2HPO_4$ (10 mM), and $KH_2PO_4$ (1.8 mM). NMR solvents, $D_3$-chloroform (99%) and $D_4$-methanol (99.5%), were purchased from Cambridge Isotope Laboratories, Inc. 2,7-Dibromo-9,9-bis(6′-bromohexyl)fluorene (**1**) was synthesized according to our previous report.[20]

**Cell Cultures.** MCF-7 breast cancer cells and NIH/3T3 fibroblast were cultured in DMEM containing 10% fetal bovine serum and 1% penicillin streptomycin at 37 °C in a humidified environment containing 5% $CO_2$. Before the experiment, the cells were precultured until confluence was reached.

**Confocal Imaging.** MCF-7 cells were cultured in the chambers (LAB-TEK, Chambered Coverglass System) at 37 °C for qualitative study. After 80% confluence, the medium was removed and the adherent cells were washed twice with 1× PBS buffer. The polymer solution (0.1 μg/mL, 0.8 mL) was then added to the chamber. After incubation for 2 h, cells were washed three times with 1× PBS buffer and then fixed by 75% ethanol for 20 min and further washed twice with 1× PBS buffer. The nuclei were stained with PI for 40 min. The cell monolayer was washed twice with 1× PBS buffer and imaged by CLSM, Zeiss LSM 410, Jena, Germany with imaging software Fluoview FV500.

**Cytotoxicity of HCPE Nanospheres.** MTT assays were performed to assess the metabolic activity of NIH/3T3 fibroblast. NIH/3T3 cells were seeded in 96-well plates (Costar, IL) at an intensity of $2 \times 10^4$ cells/mL. After 48 h incubation, the medium was replaced by **P2** solution at the concentration of 0.01, 0.02, or 0.1 mg/mL, and the cells were then incubated for 8 and 24 h, respectively. After the designated time intervals, the wells were washed twice with 1× PBS buffer and freshly prepared MTT (100 μL, 0.5 mg/mL) solution in culture medium was added into each well. The MTT medium solution was carefully removed after 3 h incubation in the incubator. Isopropanol (100 μL) was then added into each well and gently shaken for 10 min at room temperature to dissolve all the precipitate formed. The absorbance of MTT at 570 nm was monitored by the microplate reader (Genios Tecan). Cell viability was expressed by the ratio of the absorbance of the cells incubated with **P2** solution to that of the cells incubated with culture medium only.

**Synthesis of 9,9-Bis(6′-bromohexyl)-2,7-[bis(2-trimethysilyl)-ethynyl)]fluorene (2).** A solution of trimethylsilyl acetylene (1.08 g, 1.55 mL, 11.0 mmol) in $(i\text{Pr})_2\text{NH}$ (20.0 mL) was added slowly to a solution of 2,7-dibromo-9,9-bis(6′-bromohexyl)fluorene (3.25 g, 5.0 mmol), $(Ph_3P)_2PdCl_2$ (0.175 g, 0.25 mmol), and CuI (0.047 g, 0.25 mmol) in $(i\text{Pr})_2\text{NH}$ (50.0 mL) under nitrogen at room temperature. The reaction mixture was then stirred at 70 °C for 12 h. The solvent was removed under reduced pressure, and the residue was chromatographed on silica gel using hexane as eluent to give **2** (2.5 g, 75%) as white crystals. $^1$H NMR (500 MHz, $CDCl_3$, δ ppm): 7.60 (d, 2 H, $J$ = 7.8 Hz), 7.46 (dd, 2 H, $J$ = 1.2 Hz, $J$ = 7.8 Hz), 7.40 (s, 2 H), 3.28 (t, 4 H, $J$ = 6.8 Hz), 1.97−1.91 (m, 4 H), 1.70−1.60 (m, 4 H), 1.22−1.00 (m, 8 H), 0.62−0.44 (m, 4 H), 0.29 (s, 18 H); $^{13}$C NMR (125 MHz, $CDCl_3$, δ ppm): 150.53, 140.79, 131.34, 126.10, 121.88, 119.89, 105.89, 94.46, 55.07, 40.14, 33.84, 32.64, 28.99, 27.79, 23.39, 0.02; Elemental anal. Calcd (%) for $C_{35}H_{48}Br_2Si_2$: C, 61.39; H, 7.07. Found: C, 61.40; H, 7.00. MS (MALDI-TOF): $m/z$ 683.96.

(20) Pu, K. Y.; Liu, B. *Macromolecules* **2008**, *41*, 6636–6640.

**Synthesis of 9,9-Bis(6′-bromohexyl)-2,7-diethynylfluorene (3).** A KOH aqueous solution (6.0 mL, 20.0%) was diluted with methanol (25.0 mL) and added to a stirred solution of **1** (3.42 g, 5.0 mmol) in THF (50.0 mL). The mixture was stirred at room temperature for 6 h and extracted with hexane. The organic fraction was washed with water and dried over sodium sulfate. The crude product was chromatographed on silica gel using hexane as the eluent. Recrystallization of the product from methanol gave **3** (2.7 g, 90%) as white crystals. $^1$H NMR (500 MHz, $CDCl_3$, δ ppm): 7.60 (d, 2 H, $J$ = 7.8 Hz), 7.45 (dd, 2 H, $J$ = 1.3 Hz, $J$ = 7.8 Hz), 7.41 (s, 2 H), 3.24 (t, 4 H, $J$ = 6.8 Hz), 3.12 (s, 2 H), 1.98−1.85 (m, 4 H), 1.68−1.57 (m, 4 H), 1.20−0.96 (m, 8 H), 0.60−0.45 (m, 4 H); $^{13}$C NMR (125 MHz, $CDCl_3$, δ ppm): 150.65, 140.95, 131.39, 126.43, 120.97, 120.06, 84.38, 77.52, 55.07, 40.06, 33.82, 32.62, 28.99, 27.77, 23.37; Elemental anal. Calcd (%) for $C_{29}H_{32}Br_2$: C, 64.46; H, 5.97. Found: C, 64.23; H, 5.97; MS (MALDI-TOF): $m/z$ 540.20.

**Synthesis of Hyperbranched Poly[9,9-bis(6′-bromohexyl)-2,7-fluorene-*co*-phenylene] (P0).** A Schlenk tube charged with **3** (81 mg, 0.15 mmol) was degassed with three vacuum-nitrogen cycles. A solution of cyclopentadienylcobaltdicarbonyl ($CpCo(CO)_2$) in anhydrous toluene (1.5 mL, 0.01 M) was then added to the tube, and the system was further frozen, evacuated, and thawed three times to remove oxygen. The mixture was vigorously stirred at 65 °C under irradiation with a 200 W Hg lamp (operating at 100 V) placed close to the tube for 8 h. After the mixture was cooled to room temperature, it was dropped into methanol (100 mL) through a cotton filter. The precipitate was collected and redissolved in tetrahydrofuran. The resultant solution was filtered through a 0.22 μm filter and poured into hexane to further precipitate the product. After being dried in a vacuum at 40 °C, **P1** was obtained as primrose powders (52.5 mg, 65%). $^1$H NMR (500 MHz, $CDCl_3$, δ ppm): 8.4−6.5 (m), 3.62−2.94 (m), 2.27−0.398 (m); $^{13}$C NMR (125 MHz, $CDCl_3$, δ ppm): 151.50, 150.52, 142.79, 141.39, 131.35, 128.93, 126.61, 126.38, 125.28, 121.65, 120.53, 119.79, 84.54, 77.13, 55.25, 40.16, 33.80, 32.56, 29.61, 29.01, 27.72, 23.54. $M_n$ = 4500, $M_w/M_n$ = 1.7.

**Synthesis of Hyperbranced Poly[9,9-bis(6′-*N,N,N*-trimethylammonium)-hexyl)-2,7-fluorene-*co*-phenylene dibromide] (P1).** Trimethylamine (2 mL) was added dropwise to a solution of **P0** (50 mg) in THF (10 mL) at −78 °C. The mixture was stirred for 12 h, and then allowed to warm to room temperature. The precipitate was redissolved by the addition of methanol (8 mL). After the mixture was cooled to −78 °C, additional trimethylamine (2 mL) was added, and the mixture was stirred at room temperature for 24 h. After removal of the solvent, acetone was added to precipitate **P1** as yellow powders (55 mg, 95%). $^1$H NMR (500 MHz, $CD_3OD$, δ ppm): 8.35−7.06 (m, 7.15 H), 3.63 (s, 0.51), 3.30−3.20 (m, 4 H), 3.19−3.88 (br, 18 H), 2.51−1.75 (m, 4 H), 1.72−1.34 (m, 4 H), 1.31−0.87 (m, 8 H), 0.85−0.48 (m, 4 H); $^{13}$C NMR (125 MHz, $CD_3OD$, δ ppm): 151.50, 150.71, 144.27, 141.62, 140.00, 131.07, 128.82, 126.03, 124.80, 120.95, 120.45, 119.49, 88.28, 66.15, 55.18, 52.11, 39.38, 28.58, 25.20, 23.15, 22.05.

**Synthesis of P2.** A flask charged with **P1** (15 mg), PEG-$N_3$ (50 mg, 95 μmol), and CuI (1.81 mg, 9.5 μmol) was evacuated and backfilled with nitrogen. Then degassed dimethyl sulphoxide (DMSO) (1.5 mL), $H_2O$ (1.5 mL) and 1,8-diazabicyclo-[5.4.0]undec-7-ene (DBU) (1.67 mg, 9.5 μmol) were added into the flask in sequence. The reaction was conducted at 50 °C under nitrogen for 24 h. The reaction mixture was cooled to room temperature and filtered through 0.22 μm filter. The filtrate was precipitated into ether to give yellow slabby powders. The crude product was redissolved in water and further purified by

**Scheme 2. Synthesis of Core−Shell HCPE (P2)**[a]

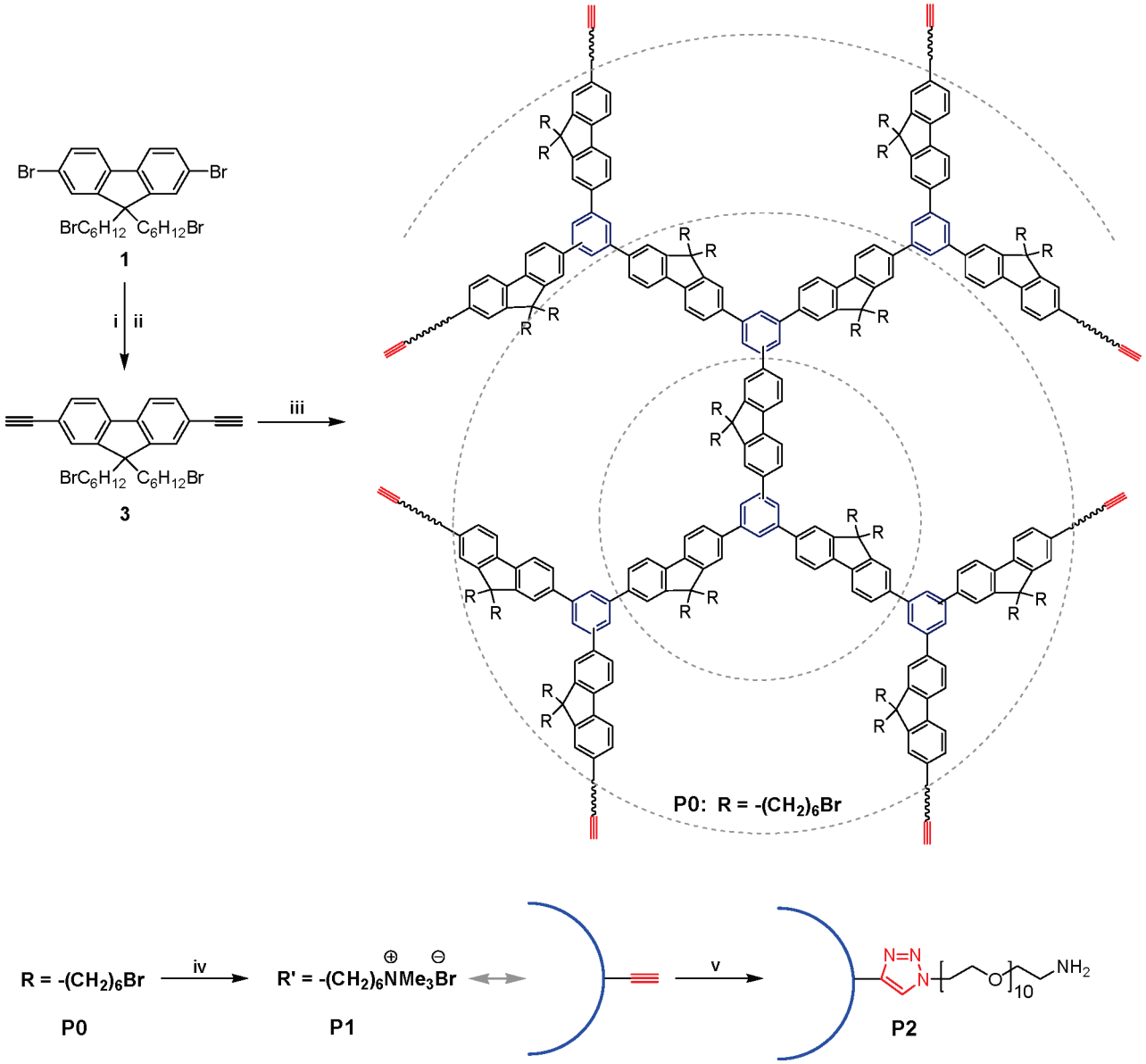


[a] Conditions and reagents: (i) trimethylsilyl acetylene, $(Ph_3P)_2PdCl_2$/CuI, $(iPr)_2NH$, 70 °C, 8 h; (ii) KOH aqueous solution, THF/$CH_3OH$, room temperature, 6 h; (iii) $CpCo(CO)_2$, toluene, 65 °C, 8 h; (iv) THF/methanol, $NMe_3$, 24 h; (v) DBU/CuI, DMSO/$H_2O$, 50 °C, 24 h.

dialysis against Mill-Q water using a 3.5 kDa molecular weight cutoff dialysis membrane for 5 days. After freeze-drying, **P2** was obtained in 78% yield as yellow powders. $^1$H NMR (500 MHz, $CD_3OD$, $\delta$ ppm): 8.54 (s), 8.40−7.37 (m), 4.69 (s), 3.99 (s), 3.83−3.45 (m), 3.29−3.11 (br), 3.10−2.75 (br), 2.62−0.38 (m).

## Results and Discussion

The synthetic route toward the HCPE is depicted in Scheme 2. 2,7-Dibromo-9,9′-bis(6-bromohexyl)fluorene (**1**) was reacted with trimethylsilyl acetylene in a standard $(Ph_3P)_2PdCl_2$/CuI catalyzed Sonagashira coupling reaction to afford 9,9-bis(6′-bromohexyl)-2,7-[bis(2-trimethysilyl)-ethynyl)]fluorene (**2**).[21] The diyne monomer, 9,9′-bis(6-bromohexyl)-2,7-diethynylfluorene (**3**), was obtained from deprotecting the trimethylsilyl groups of **2** in a basic solution. The correct structure and purity of **3** were determined by NMR, mass spectrum and elemental analysis. Homopoly-cyclotrimerization of **3** was conducted in anhydrous toluene using 10 mol % $CpCo(CO)_2$ as the catalyst under UV radiation in nitrogen atmosphere. The resultant neutral hyperbranched conjugated polymer (**P0**) natively has the alkyne groups as the end-capper, allowing subsequent click reaction with azide compound. Considering the higher reaction efficiency of click reaction in aqueous solution relative to that in organic solvents,[18] quaternization of **P0** to its water-soluble cationic counterpart (**P1**) was conducted before the click reaction. Treatment of **P0** with trimethylamine in THF/methanol mixture yielded **P1** in a high yield of 95%.[22]

(21) (a) Pu, K. Y.; Pan, S. Y. H.; Liu, B. *J. Phys. Chem. B* **2008**, *112*, 9295–9300. (b) Pu, K. Y.; Qi, X. Y.; Yang, Y. L.; Lu, X. M.; Li, T. C.; Fan, Q. L.; Wang, C.; Liu, B.; Chan, H. S. O.; Huang, W. *Chem.—Eur. J.* **2008**, *14*, 1205–1215.

(22) (a) Pu, K. Y.; Fang, Z.; Liu, B. *Adv. Funct. Mater.* **2008**, *18*, 1321–1328. (b) Pu, K. Y.; Liu, B. *Adv. Funct. Mater.* **2009**, *19*, 1371–1378. (c) Pu, K. Y.; Zhan, R.; Liu, B. *Macromol. Symp.* **2009**, *279*, 48–51.

Finally, copper-catalyzed Huisgen cycloaddition was used to attach PEG to the periphery of **P1**. The reaction was performed between **P1** and azide-functionalized PEG ($N_3$−PEG) at 50 °C under nitrogen in the mixture of DMSO/water (1:1) using DBU and CuI as the catalyst. The resultant core−shell HCPE (**P2**) was purified by precipitation, microfiltration, and finally dialysis against Mill-Q water for 5 days using a 3.5 kDa molecular weight cutoff dialysis membrane.

The chemical structures of **P0**−**P2** are characterized by NMR. Although the proton resonance peak of alkyne end-cappers (−C≡C<u>H</u>) in the $^1$H NMR of **P0** overlaps with that of −$CH_2C\underline{H}_2$Br, it becomes visible in the $^1$H NMR of **P1**, which allows estimation of the degree of polymerization (DP). In the $^1$H NMR of **P1**, the ratio of the integrated area of the peak at 3.63 ppm (corresponding to the proton resonance of end-capping alkynes) to that of the peak at 0.66 ppm (corresponding to the proton resonance of methylene groups in fluorene) is ∼0.135, indicating that the DP is ∼18. Accordingly, the number-average molecular weight of **P0** can be estimated to be ∼10 000. The successful click reaction between **P1** and $N_3$−PEG is confirmed by the disappearance of the alkyne peak at 3.63 ppm and the appearance of the peak at 8.53 ppm assigned to the proton resonance of triazole group (−NC<u>H</u>=C−).

The normalized UV−vis absorption and PL spectra of **P1** and **P2** in 15 mM phosphate-buffer saline (PBS, pH 7.4) are shown in Figure 1. **P1** and **P2** have absorption maxima at 355 and 361 nm, respectively. The red-shifted absorption maximum of **P2** relative to **P1** indicates that the electron-delocalized triazole units introduced by click reaction also contribute to the effective conjugation length of **P2**. On the other hand, both **P1** and **P2** exhibit featureless PL spectra with emission maxima at 409 and 415 nm, respectively, which coincides well with their irregular stereostructures. The PL quantum yields of **P1** and **P2** in 15 mM PBS are 0.40 and 0.30, respectively, measured using quinine sulfate in 0.1 M $H_2SO_4$ (quantum yield = 0.55) as the reference. The lower quantum yield of **P2** relative to **P1** could be ascribed to the electron-deficient triazole units within **P2**, which slightly quench the polymer fluorescence through charge transfer.[23] However, in 150 mM PBS, the PL quantum yield decreases substantially for **P1** (0.20), whereas it changes only slightly for **P2** (0.28). The high fluorescence of **P2** at elevated ionic strength should benefit from its hydrophilic PEG shell that protects the conjugated core from aggregation. As a result, **P2** is more promising than **P1** for biological application, wherein environmenally sustainable fluorescence is a basic precondition.

Because hyperbranched aromatic polymers have three-dimensional nanostructures,[13,14] the molecular size of **P1** and **P2** in pure water can be measured by dynamic light scattering (DLS). The polymer concentration for DLS is

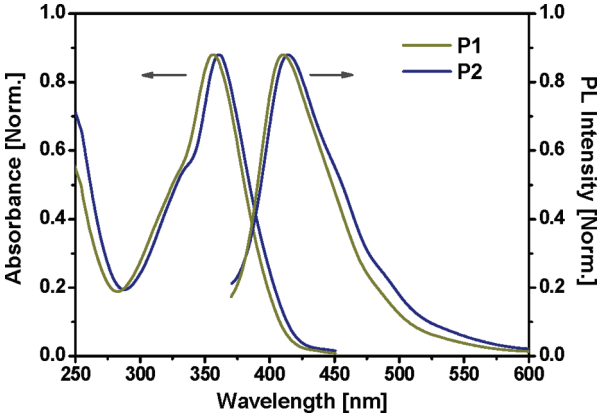


**Figure 1.** Normalized UV−vis absorption and PL spectra of **P1** and **P2** in 15 mM PBS at pH 7.4 (excitation at 355 nm).

0.1 μg/mL. Unimodal scattering peak is observed for both polymer solutions (Figure S1 in the Supporting Information), showing that the average diameters of the particles in **P1** and **P2** solutions are 10.8 ± 1.4 and 13.5 ± 1.2 nm, respectively. Because the DP for the conjugated segments of **P1** and **P2** is ∼18, the average diameter of the conjugated segments with a favorite conformation is ∼8 nm as calculated from molecular simulation. Considering the extremely low concentration of polymer solutions, the obtained particle size from DLS-measurement should be similar to that of the single-molecular nanosphere for **P1** and **P2**. The larger particle size of **P2** relative to that of **P1** is ascribed to the extra PEG shell of **P2**. When the same measurement is done in 25 mM PBS buffer, the average diameter of **P1** increases to 60 ± 2.5 nm, indicating the formation of polymer aggregates. In contrast, the average diameter of **P2** is nearly the same in buffer (14.2 ± 1.3 nm) as compared to that in pure water, which originates from the protection of its hydrophilic PEG shell. These phenomena accord well with the effect of ionic strength on PL quantum yields of **P1** and **P2**, revealing the good stability of the single-molecular nanoparticles of **P2** in buffer.

The molecular morphology of **P2** in dry state is studied by HR-TEM. The sample was prepared by drop-coating the polymer aqueous solution (0.1 μg/mL) onto cupper grid, followed by freeze-drying. This sample preparation process is well-known to greatly maintain the polymer morphology in solution.[24] As shown in Figure 2a, **P2** forms uniform nanospheres. In addition, these nanospheres possess a core−shell structure (Figure 2b), wherein the dark interior and the gray exterior correspond to the areas enriched with the conjugated segments and the saturated PEG peripheries, respectively. The elemental composition of these nanospheres is probed by in situ energy-dispersive X-ray (EDX) analysis, showing the consistency with the chemical structure of **P2** (Figure S2 in the Supporting Information). Statistical calculation of 305 nanospheres (Figure 2c) indicates that the average diameter and the polydispersity of **P2** nanospheres are

(23) (a) Yamamoto, T.; Sugiyama, K.; Kushida, T.; Inoue, T.; Kanbara, T. *J. Am. Chem. Soc.* **1996**, *118*, 3930–3937. (b) Pu, K. Y.; Liu, B. *Adv. Funct. Mater.* **2009**, *19*, 277–284.

(24) Schacher, F.; Walther, A.; Ruppel, M.; Drechsler, M.; Müller, A. H. E. *Macromolecules* **2009**, *42*, 3540–3548.

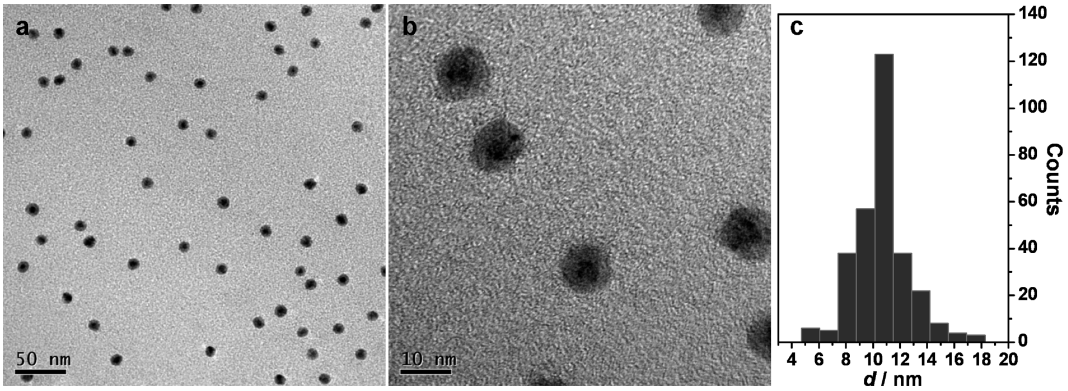


**Figure 2.** (a, b) HR-TEM images and (c) size distribution histogram of the HCPE nanoparticles.

~10.7 nm and 1.50, respectively. The size measured from TEM is slightly smaller than that obtained from DLS, which should be caused by the shrinkage of the flexible PEG chains of **P2** during drying process. However, it is clear that the majority of these nanospheres consist of a single molecule of **P2**. The single-molecular nanospherical structure of **P2** arises from the rigid conjugated core that offers shape persistence, and the nonionic water-soluble PEG shells that passivate the molecular surface and exclude strong intermolecular interactions.[25] In addition, such core−shell structure of single-molecular nanospheres of HCPE is beneficial to cell imaging, as PEG shells can reduce the nonspecific adsorption of the nanospheres.

To demonstrate the applicability of **P2** in biological imaging, we applied HCPE nanospheres to visualize breast cancer cells (MCF-7) in vitro. After incubation with the HCPE nanosphere solution (0.1 $\mu$g/mL) for 2 h, MCF-7 cells were fixed and their nuclei were stained with propidium iodide (PI). The relatively strong PL intensity of HCPE ranging from 450 to 500 nm allows collecting green fluorescent signal. The confocal laser scanning microscopy (CLSM) images of the sample are displayed in Figures 3a and 3b, corresponding to the fluorescence image and fluorescence/transmission overlapped image, respectively. It is noteworthy that there is no observable cellular autofluorescence under the same CLSM parameters used for Figure 3 (see Figure S3 in the Supporting Information). Although PEG is known to reduce the immunogenicity and nonspecific uptake of nanoparticles, this effect is strongly dependent on the molecular weight of PEG, and PEG with a molecular weight less than 2KDa was reported to show no effect on cellular uptake process both in vitro and in vivo.[26] Because the PEG segment of **P2** is very short (0.5 KDa), it should not affect the cellular uptake. As shown in images a and b in Figure 3, HCPE nanospheres are efficiently internalized by MCF-7 cells and accumulated in the cytoplasm. However, under the same conditions, the CLSM images of MCF-7 cells incubated with **P1** solution show

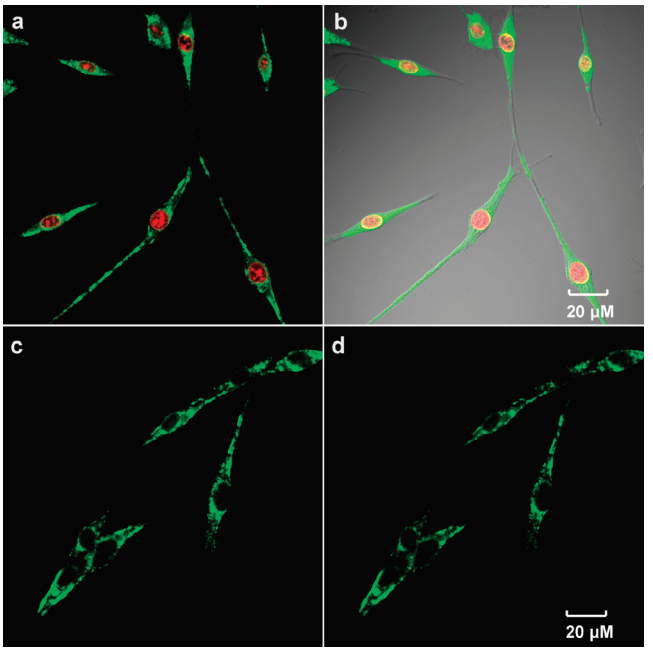


**Figure 3.** CLSM (a) fluorescence image and (b) fluorescence/transmission overlapped image of MCF-7 cells costained by **P2** and **P1**; time-resolved CLSM fluorescence images of MCF-cells stained by **P2** under laser scanning for (c) 0 min and (d) 15 min.

relatively weak fluorescence and the **P1** particles are not evenly distributed in the cell cytoplasm (Figure S4 in the Supporting Information). The difference in the CLSM images between **P1** and **P2** reveals that the cellular uptake of **P1** is less efficient than that of **P2**, which should result from the aggregation for **P1** in biological media. In addition, because the average diameter of the HCPE nanospheres is less than 25 nm (~10.7 nm), **P2** molecules should transport to the cytoplasm through a cholesterol-independent and nonclathrin- and noncaveolae-mediated endocytosis mechanism according to the previous report on polymeric particles.[27] This is supported by the nearly homogeneous distribution of the HCPE nanospheres in the cell cytoplasm. Moreover, the fluorescence from the HCPE nanospheres in the cytoplasm is as strong as that from PI in the nuclei, which enables us to observe the entire cellular structure in a clear and bright manner.

(25) Sheiko, S. S.; Möller, M. *Curr. Top. Chem.* **2001**, *212*, 137–175.
(26) (a) Liu, Z.; Winters, M.; Holodniy, M.; Dai, H. *Angew. Chem., Int. Ed.* **2007**, *46*, 2023–2027. (b) Zeineldin, R.; Al-Haik, M.; Hudson, L. G. *Nano Lett.* **2009**, *9*, 751–757.
(27) Lai, S. K.; Hida, K.; Man, S. T.; Chen, C.; Machamer, C.; Schroer, T. A.; Hanes, J. *Biomaterials* **2007**, *28*, 2876–2884.

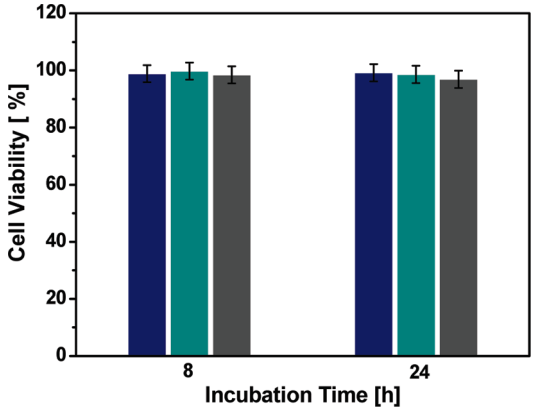


**Figure 4.** In vitro viability of NIH 3T3 cells treated with the HCPE nanosphere solutions at the concentration of 0.01 (blue), 0.02 (cyan), or 0.1 mg/mL (gray) for 8 and 24 h. The percentage cell viability of treated cells is calculated relative to that of untreated cells with a viability arbitrarily defined as 100%.

The photostability of HCPE nanospheres in cells under CLSM scanning was also investigated. As shown in images c and d in Figure 3, the fluorescence intensity decreases less than 10% after continuous laser scanning for 15 min, indicating good photostability of HCPE nanospheres. The performance of HCPE nanospheres is thus superior to many commercial dyes (such as fluorescein, rhodamine, and Cy5) which usually lose their fluorescence within 1−3 min under similar CLSM laser radiation conditions.[28] The good photostability of HCPE nanospheres should be partially ascribed to the PEG shells that prevent the luminescent conjugated core from intensive contact with oxygen-rich environment. Additionally, the intrinsic photostability of hyperbranched conjugated polymers is also contributive.[15,16]

As biocompatibility plays an essential role in the long-term clinical applications of fluorescent nanomaterials, the cytotoxicity of HCPE nanospheres is evaluated for mouse embryonic fibroblast cells (NIH 3T3) using MTT cell-viability assay. Figure 4 summarizes the in vitro NIH 3T3 cell viability after being cultured with the nanosphere solutions at the concentration of 0.01, 0.02, or 0.1 mg/mL for 8 or 24 h. It is noteworthy that these nanosphere concentrations are much higher than that used for practical cell imaging (0.1 $\mu$g/mL). Within the tested period, the cell viabilities are close to 100%, indicating that the HCPE nanospheres have low cytotoxicity. This result is consistent with the previous studies where conjugated polymers (such as polyaniline, polypyrrole, and polythiophene derivatives) are used as electroactive biomaterials in tissue engineering applications.[29]

## Conclusion

In conclusion, we take advantage of polycyclotrimerization in conjunction with alkyne-azide "click" chemistry to construct a water-soluble hyperbranched conjugated polymer. This polymer has a double-layered ingredient architecture, which intrinsically forms single-molecular core−shell nanospheres with an average diameter of ~10.7 nm and a size distribution of ~1.5 as drawn from TEM images. The inherent water miscibility and hyperbranched inner architecture endow HCPE-based nanospheres with high PL quantum yield in buffer solution (0.30), allowing visualizing cellular structure in an efficient and bright fashion. More importantly, by virtue of the PEG shells, these single-molecular nanospheres possess good photostability and cytocompatibility, demonstrating a great potential in long-term clinical applications.

In view of the state-of-the-art synthetic methods used herein, the hyperbranched conjugated core is naturally studded with alkyne active groups, providing the feasibility and flexibility to modify the shell component with diverse biocompatible materials or recognition elements through subsequent click chemistry for specific biological applications. In addition, the size of HCPE-based nanospheres can also be desirably adjusted by using shell segments with different length or cores of different generation. As a result, this investigation highlights the opportunities of exerting core−shell hyperbranched architecture to bring conjugated polymers into biological imaging.

**Acknowledgment.** The authors are grateful to the National University of Singapore (ARF R-279-000-234-123) and Singapore Ministry of Education (R-279-000-255-112) for financial support. We also thank Prof. S. S. Feng for providing the facilities for cell culture.

**Supporting Information Available:** DLS plots of the polymers in water, EDX of the HCPE nanospheres, and CLSM images of free MCF-7 cells and **P1**-stained MCF-7 cells (PDF). This material is available free of charge via the Internet at http://pubs.acs.org.

(28) Resch-Genger, U.; Grabolle, M.; Cavaliere-Jaricot, S.; Nitschke, R.; Nann, T. *Nat. Methods* **2008**, *5*, 763–775.

(29) Guimard, N. K.; Gomez, N.; Schmidt, C. E. *Prog. Polym. Sci.* **2007**, *32*, 876–921.